OPEN ACCESS Freely available online

PLOS ONE

Overexpression of Extracellular Superoxide Dismutase Protects against Brain Injury Induced by Chronic Hypoxia

Nahla Zaghloul[1], Hardik Patel[7], Champa Codipilly[7], Philippe Marambaud[2], Stephen Dewey[3], Stephen Frattini[4], Patricio T. Huerta[4,5], Mansoor Nasim[6], Edmund J. Miller[5,7], Mohamed Ahmed[1,7]*

1 Division of Neonatal-Perinatal Medicine, The Ohio State University and Nationwide Children's Hospital, Columbus, Ohio, United States of America, **2** Laboratory of Memory Disorders, Feinstein Institute for Medical Research, Manhasset, New York, United States of America, **3** Neuroimaging Department, Feinstein Institute for Medical Research, Manhasset, New York, United States of America, **4** Laboratory of Immune & Neural Networks, Feinstein Institute for Medical Research, Manhasset, New York, United States of America, **5** Department of Molecular Medicine, Hofstra North Shore LIJ School of Medicine, New York, United States of America, **6** Department of Pathology, NSL-IJ, Manhasset, New York, United States of America, **7** Division of Neonatal-Perinatal Medicine, Cohen Children's Medical Center of New York and Lilling Family Research laboratory, Feinstein Institute for Medical Research, Manhasset, New York, United States of America

Abstract

Extracellular superoxide dismutase (EC-SOD) is an isoform of SOD normally found both intra- and extra-cellularly and accounting for most SOD activity in blood vessels. Here we explored the role of EC-SOD in protecting against brain damage induced by chronic hypoxia. EC-SOD Transgenic mice, were exposed to hypoxia (FiO2.1%) for 10 days (H-KI) and compared to transgenic animals housed in room air (RA-KI), wild type animals exposed to hypoxia (H-WT or wild type mice housed in room air (RA-WT). Overall brain metabolism evaluated by positron emission tomography (PET) showed that H-WT mice had significantly higher uptake of ^{18}FDG in the brain particularly the hippocampus, hypothalamus, and cerebellum. H-KI mice had comparable uptake to the RA-KI and RA-WT groups. To investigate the functional state of the hippocampus, electrophysiological techniques in *ex vivo* hippocampal slices were performed and showed that H-KI had normal synaptic plasticity, whereas H-WT were severely affected. Markers of oxidative stress, GFAP, IBA1, MIF, and pAMPK showed similar values in the H-KI and RA-WT groups, but were significantly increased in the H-WT group. Caspase-3 assay and histopathological studies showed significant apoptosis/cell damage in the H-WT group, but no significant difference in the H-KI group compared to the RA groups. The data suggest that EC-SOD has potential prophylactic and therapeutic roles in diseases with compromised brain oxygenation.

Citation: Zaghloul N, Patel H, Codipilly C, Marambaud P, Dewey S, et al. (2014) Overexpression of Extracellular Superoxide Dismutase Protects against Brain Injury Induced by Chronic Hypoxia. PLoS ONE 9(9): e108168. doi:10.1371/journal.pone.0108168

Editor: Tim D. Oury, University of Pittsburgh, United States of America

Received May 2, 2014; **Accepted** August 19, 2014; **Published** September 30, 2014

Data Availability: The authors confirm that all data underlying the findings are fully available without restriction. All relevant data are within the paper.

Funding: The author(s) received no specific funding for this work.

Competing Interests: The authors have declared that no competing interests exist.

* Email: mahmed2@nshs.edu

Introduction

Hypoxia plays a crucial role in acute and chronic CNS pathologies. Exposure to hypoxia results in a significant increase in reactive oxygen species (ROS), including superoxide, which is produced mainly in the mitochondria [1–4]. ROS leads to impaired neurogenesis, hippocampal atrophy, altered transcription factor regulation, and protein expression [5–6].

Excess ROS, particularly superoxide, can oxidize nitric oxide (NO) to reactive nitrogen species (RNS) including peroxynitrite [7–8]. This process leads to decreased NO bioavailability, accumulation of toxic products including NO2 [9–10]. Both ROS and RNS oxidize macromolecules (DNA, proteins, and lipids), culminating in CNS neurodegeneration [11]. Oxidative stress also activates glial-mediated inflammation [12]. HIF-1 alpha rapidly accumulates during the onset of hypoxia, remaining at this level for 14 days before gradually declining to normal by 21 days despite continuous hypoxia [13–14]. A pathophysiological role for HIF-1alpha has been established for hypoxic ischemic diseases [15].

Neurons are particularly susceptible to ROS/RNS injury [16], but may adapt to hypoxia by activating neuroprotective signaling cascades e.g. MAPK, ERK1/2, and protein kinase-B [17–18] increasing glycolytic energy metabolism and free-radical defenses [19], down-regulating oxidative-stress genes, and up-regulating antioxidant genes [20].

Overexpression of mitochondrial SOD2 inhibits post-ischemic mitogen-activated protein kinase and decreases DNA fragmentation following ischemia/reperfusion [21–25]. The outcome from middle cerebral artery occlusion is worse in SOD2 deficient animals [26]. A neuroprotective role for SOD mimetics has been demonstrated in an *ex-vivo* brain model [27].

EC-SOD is expressed in the brain at a lower level than other SODs [28], but provides defense against ROS produced by membrane-bound NAD(P)H oxidase [29]. EC-SOD is predominantly localized in neurons of hippocampus, lateral nucleus of the thalamus and hypothalamus. Both EC-SOD and neuronal NO synthase are similarly distributed in the striatum and cortex [30]. EC-SOD is the only extracellular SOD isoform and the major SOD activity in blood vessels, which leads to increase NO bioavailability [31].

Mice, engineered to overexpress EC-SOD, have increased tolerance to both focal and global cerebral ischemia [32–34], while EC-SOD knock-outs exhibit enhanced damage [35]. These data implicate an important role for EC-SOD ischemia/reperfusion pathologies, and suggest a therapeutic role for SOD mimetics.

Previously, we showed that EC-SOD offers significant protection against oxidative stress-induced lung injury [36–37] and brain injury induced by hyperoxia [38]. In this study, we hypothesized that EC-SOD overexpression offers protection to the brain exposed to chronic hypoxia. This could be of importance to many diseases with compromised brain oxygenation.

Material and Methods

All experiments involving animals were reviewed and approved by the Institutional Animal Care and Use Committee of the Feinstein Institute for Medical Research, and performed in accordance with the guidelines set by the Institute for Laboratory Animal Research. Adult C57BL6 mice, (8–10 week old), either wild type (WT) or transgenic animals (KI) generated by microinjecting nuclei of fertilized oocytes from (C57Bl/6#C3H), with the cDNA of human EC-SOD containing a Beta-actin promoter [29], were housed in a pathogen-free environment, under standard light and dark cycles, with free access to food and water. An animal hypoxia chamber system (BioSpherix, Lacona, NY) was used for the *in vivo* studies. With this system, a constant 10% normobaric hypoxia was achieved for up to 10 days in our study. Animals were divided into four groups (10/group) and housed for 10 days as follows: Group A: WT adult mice housed in room air (RA-WT). Group B: KI adult mice housed in room air (RA-KI). Group C: WT adult mice housed in hypoxia (H-WT). Group D: KI adult mice housed in hypoxia (H-KI). After 10 days, the animals were assessed using PET, and were then euthanized and brain tissues harvested.

Functional studies

1- PET scanning. Brains were scanned after exposure to hypoxia for 10 days and compared to matched room air controls. Scanning was performed using ^{18}FDG, which was injected intraperitoneally at a dose of 400 Micro Curie per mouse. After 45 min., the mice were assessed at the PET scan center located within the Feinstein Institute for Medical Research.

2- Hippocampal Electrophysiology. Mice were anesthetized with isoflurane in a closed container, then immediately decapitated. The brain was quickly extracted into ice-cold (<2C) artificial cerebral spinal fluid (ACSF) that contained: NaCl (126 mM), $NaHCO_3$ (26 mM), glucose (10 mM), KCl (2.5 mM), $CaCl_2$ (2.4 mM), $MgCl_2$ (1.3 mM), and NaH_2PO_4 (1.2 mM), and was continuously gassed with carbogen (95% O_2, 5% CO_2). Kynurenic acid (1 mM), which is a non-specific blocker of excitatory amino acid receptors, was added to the ACSF solution during the dissection and slicing procedures. The brain was bisected and both hemispheres were mounted onto a block with ethyl cyanoacrylate glue. Transverse hippocampal slices (400 mm thick) were prepared using a Leica VT1200 vibratome. Slices were incubated in ACSF gassed with carbogenfor 35 min at 35C followed by 120 min at 24C. One slice at a time was transferred to a recording chamber, continuously perfused with ACSF gassed with carbogen at 30C, for electrophysiological studies. Field excitatory postsynaptic potentials (fEPSP) were recorded with borosilicate glass electrodes (2–3 M ohmns tip resistance) placed in the stratum radiatum, of the CA1, at the midpoint between two bipolar stimulating electrodes (Frederick Haer & Co, Bowdoinham, ME) that activated Schaeffer collateral/commissural axons. This setup allowed for the recording of two independent pathways (test and control) in the same slice. The initial slope of the fEPSP was used as a measure of the postsynaptic response. fEPSP responses were amplified (AM Systems 1800), digitized at 10 kHz, and analyzed online with custom software (written with AxoBasic, Axon Instruments, Union City, CA). For obtaining input-output (I-O) functions, the stimulation was reduced to a value at which no fEPSP was evoked. The stimulation was then increased incrementally to evoke larger fEPSPs. This was done until the appearance of a population spike, generated by CA1 pyramidal cells, which defined the final point of the I-O function. For plasticity experiments, a stable baseline was obtained for at least 15 min. The baseline intensity was set to obtain a fEPSP slope that was half-maximal, as determined by I-O curves. Long-term potentiation (LTP) was induced by high-frequency stimulation (HFS), which consisted of either tetanus (100 Hz for 1 sec) or theta burst stimulation (TBS, 10 trains of 4 pulses at 100 Hz, with 200 ms between trains). We calculated LTP from 30 responses at 40–45 min post-HFS. For all LTP experiments, picrotoxin (100 microM) was added to block $GABA_A$ receptors [39].

Molecular studies

1- Superoxide dismutase (SOD) assays. After PET scanning, all animals were euthanized. Brains were isolated and immediately frozen. SOD activity was assessed in brain homogenates using an Oxiselect superoxide dismutase activity assay kit (Cell Biolabs, Dan Diego, CA). This assay utilizes a xanthine/xanthine oxidase system to generate superoxide anions, which reduce a chromagen to a water soluble formazan dye. The activity of SOD in the brain tissue homogenate was determined as the inhibition of chromagen reduction. Quantitative assays of SOD1, SOD2,and hSOD3 were done by western blot and compared to B-Actin protein concentration.

2- Glutathione assay. For the determination of the reduced glutathione (GSH) and oxidized glutathione (GSSG) ratio, the brain was homogenized and the homogenates were treated with a mixture of metaphosphoric acid, EDTA, and NaCl. After centrifugation, aliquots were taken for neutralization with disodium hydrogen phosphate followed by addition of DTNB. Reduced and oxidized glutathione were measured in brain tissue homogenates by reaction with DTNB (5,5′-dithiobis-2-nitrobenzoic acid) using a Glutathione Assay Kit (Calbiochem, Gibbsontown, NJ), following the manufacturer's instructions. Reduced glutathione (GSH) was determined after reaction with DTNB in a spectrophotometer at 412 nm. For the determination of oxidized glutathione (GSSG), the autoxidation of GSH was stopped by addition of N-ethylmaleimide. After addition of sodium hydroxide, GSSG was modified using o-phthalaldehyde. GSSG was determined at a spectrofluorometer (excitation: 350 nm, emission: 420 nm) using GSSG standards for quantification [40].

3- Western Blotting. Frozen brain tissues were crushed and homogenized, and protein extraction was carried out using a Total Protein Extraction Kit (BioChain Institute, Inc. Hayward, CA). Protein concentration was estimated using the Modified Lowry Protein Assay (Thermo Fisher Scientific, Rockford, IL, USA). Samples were prepared for SDS-PAGE in Laemmli Sample Buffer (Bio-rad, Hercules, CA, USA). Standard SDS-PAGE techniques were followed as previously described [38]. Running buffer and Transfer buffer were purchased from Bio-Rad (Hercules, CA, USA). Briefly electrophoresis was performed using a Mini Format 1-D Electrophoresis Systems (Bio-Rad, Hercules, CA, USA) on 10–12% ready tris-HCl gels (Bio-rad, Hercules, CA, USA). After electrophoresis, proteins were transferred to a PVDF membrane using a Wet/Tank Blotting System (Bio-rad, Hercules, CA, USA).

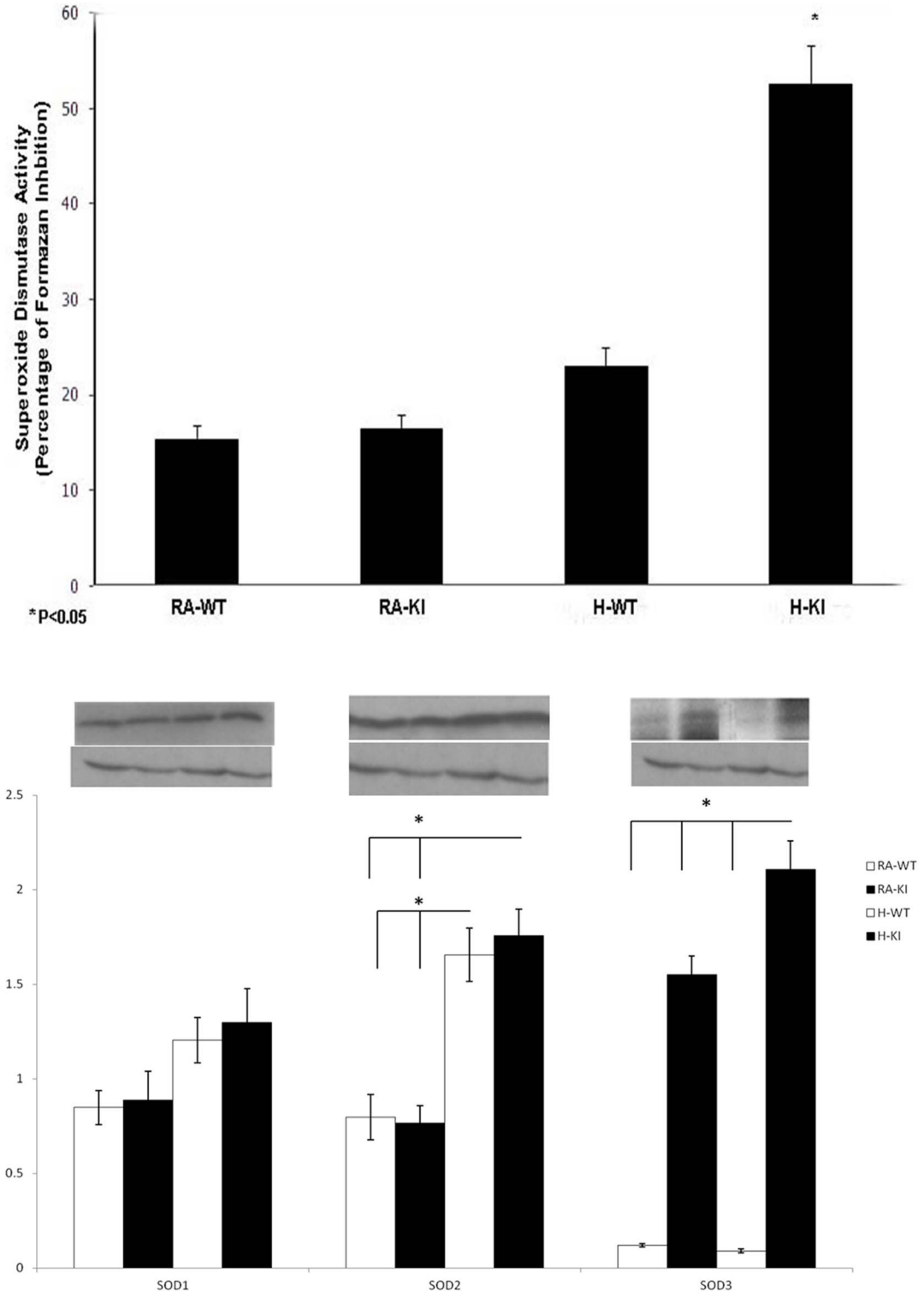

Figure 1. SOD activity ratio in adult mouse brain groups (WT and KI), after exposure to hypoxia (10% for 10 days) in comparison with the RA control groups (WT and KI). Data are mean of 10 animals per group ± SEM. *P<0.05 versus the KI hypoxia and WT hypoxia groups **(Fig. 1A).** Quantitative Western blot for SDO1, SOD2 & hSDO3 (presented as a ratio for B-Actin), in adult mouse brain groups (WT and KI) after exposure to hypoxia (10% for 10 days) in comparison with the RA control groups (WT and KI). Data are mean of 5± SEM animals per group. *P<0.05 HI-KI vs. RA groups and WT hypoxia groups; and H-WT vs. RA groups **(Fig. 1B)**.
doi:10.1371/journal.pone.0108168.g001

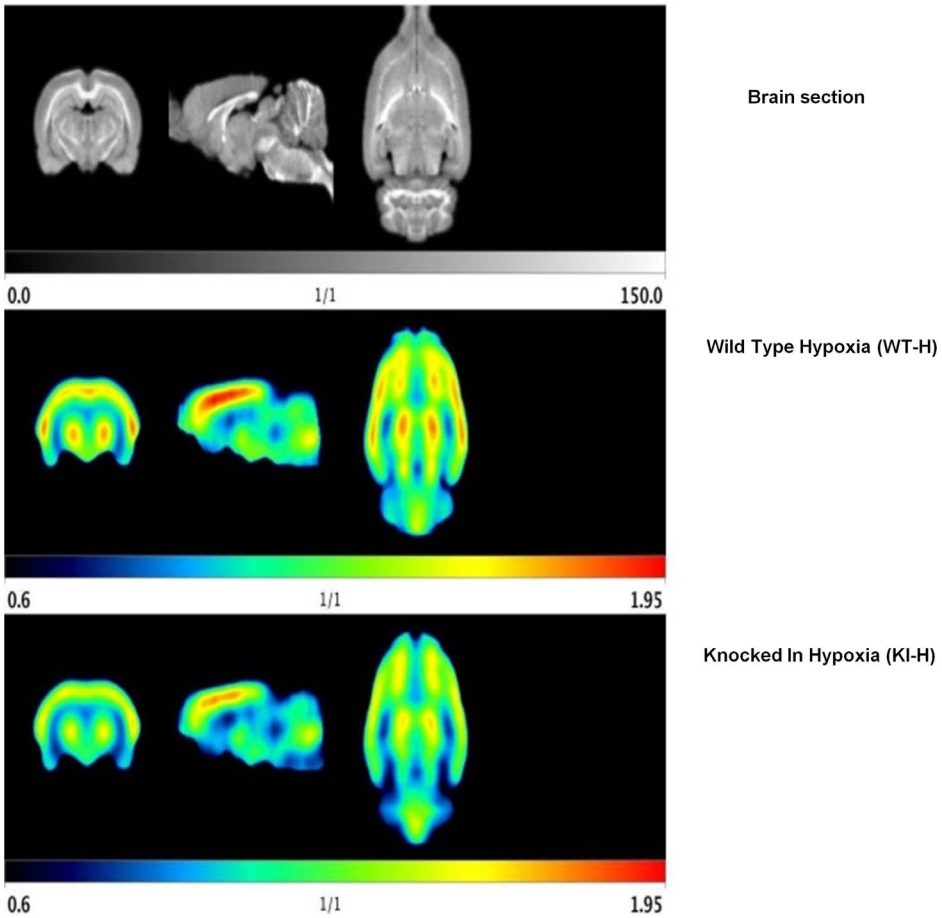

Figure 2. Brain PET scan with an FDG standardized uptake value, showing a cross and longitudinal sections of brain uptake.
doi:10.1371/journal.pone.0108168.g002

Membranes were briefly washed and immediately incubated with respective primary antibody in 5% BSA with PBST overnight (primary antibody was diluted according to the manufacturer's recommendation). The next day, after washing, the membranes were incubated with HRP-conjugated secondary antibodies for 40–60 min (diluted according to the manufacturer's recommendation). After incubation with secondary antibody, the membranes were washed and then processed using Amersham ECL detection systems (GE healthcare, Piscataway, NJ USA). The membranes were then immediately exposed to 8×10 Fuji X-Ray Film. Developed films were quantified using Quantity One 1-D Analysis Software on a GS-800 Calibrated Densitometer. The density of each band was evaluated and presented as a ratio in comparison to Actin band density. The following primary antibodies were used to detect the following markers: GFAP (Cell Signaling Technology, Danvers, MA, USA), Iba-1 (Wako Chemicals USA, Richmond, VA, USA), MIF (Abcam, Cambridge, MA, USA), pAMPK (Beauchamp et al., 2004), (Cell Signaling Technology, Danver, MA), pAMPK (Cell Signaling Technology, Danver, MA, USA), and anti-Actin protein (as an internal control) (Gene Script, Olathe, KS, USA). Horseradish Peroxidase (HRP)-Conjugated Goat Anti-Rabbit IgG conjugate was used for detection of rabbit primary antibodies (Bio-Rad, Hercules, CA, USA). Goat anti-mouse HRP conjugates were used for detection of mouse primary antibodies (Southern Biotech, Birmingham, AL, USA).

Structural studies

1- Caspase 3 activity assay. Caspase 3 activity was measured using the Caspase-3 Colorimetric Assay (R&D Systems, Minneapolis, MN, USA). The assay was carried out following the manufacturer's instructions and described previously [41]. Brain tissue samples were homogenized in buffer containing 10 mM HEPES (pH 7.4), 42 mM KCl, 5 mM MgCl2, 1 mM dithiothreitol, 1% Triton X-100, 0.5% CHAPS, 1 mM phenyl methyl sulfonyl fluoride, and 1 micro gm/mL leupeptin, and centrifuged at 12,000 *g* for 10 minutes at 4°C. A 10-µL aliquot of the lysate was incubated in a flat bottom 96 well plate, 50 microL tissue lysates were incubated with 50 microL 2x reaction buffer followed by 5 microL of caspase-3 colorimetric substrate (DEVD-pNA), and incubated at 37C for 2 hrs. The fluorescence was measured at room temperature at the excitation wavelength of 360 nm, and emission was measured at 460 nm with the use of a multiplate fluorescence reader (Biotek Instruments). Protein concentration was measured with a Pierce kit (Pierce Biotechnology, Rockford, IL, USA). Ac-AMC was used to obtain a standard curve. Enzyme activity was calculated as picomoles per minute per mg of protein.

2- Histopathological studies. Brain tissue was fixed in 10% neutral buffered formalin for 24 hours, processed, embedded in paraffin wax, and subsequently cut into 4 micron thick sections. Following de-paraffinization, hematoxylin and eosin (H&E) staining was performed according to standard protocols. Standard sections were made of the hippocampus, cerebellum, and cerebrum in each group of animals.

Table 1. PET scan data showing FDG in adult mice brain groups (WT and KI) after exposure to hypoxia (10% for 10 days), in comparison with the RA control groups (RA-WT and RA-KI).

Region	RA-WT	RA-KI	H-WT	H-KI	*P value
AcbCore/Shell	0.442	0.436	1.494	0.940	0.003
CaudatePutamen	0.513	0.494	1.727	1.056	0.006
CentralCanal-PAG	0.401	0.396	1.480	0.961	0.004
Pons	0.159	0.156	0.635	0.382	0.004
Septum	0.385	0.372	1.423	0.893	0.001
Medulla	0.220	0.207	0.842	0.490	0.005
Whole Brain	0.349	0.326	1.237	0.754	0.001
Amygdala	0.222	0.209	0.741	0.447	0.002
Cortex-Auditory	0.488	0.450	1.599	0.937	0.002
Cingulate-Ctx	0.607	0.540	2.019	1.223	0.001
Entorhinal-Ctx	0.206	0.195	0.675	0.409	0.003
Frontal-Ctx	0.459	0.355	1.641	0.993	0.002
Insular-Ctx	0.346	0.318	1.218	0.731	0.001
MedialPrefrontal-Ctx	0.558	0.525	1.827	1.130	0.003
Motor-Ctx	0.543	0.447	1.958	1.152	0.001
OrbitoFrontal-Ctx	0.500	0.440	1.802	1.123	0.000
Parietal-Ctx	0.532	0.456	1.809	1.113	0.001
Retrosplenial-Ctx	0.548	0.486	1.871	1.113	0.002
Somatosensory-Ctx	0.539	0.480	1.881	1.132	0.002
Visual-Ctx	0.520	0.471	1.752	1.049	0.001
Hippocampus-Dorsal	0.412	0.381	1.426	0.921	0.003
Hippocampus-Ventral	0.340	0.316	1.277	0.813	0.002
Hypothalamus	0.183	0.177	0.687	0.411	0.001
Olfactory-Ctx	0.248	0.235	0.907	0.581	0.000
pituitary	0.001	0.001	0.005	0.003	0.004
Superior Colliculi	0.519	0.467	1.712	1.061	0.000
Midbrain	0.457	0.441	1.605	0.966	0.003
VTA	0.304	0.310	1.121	0.677	0.005
Cerebellar Grey	0.323	0.321	1.151	0.699	0.008
Cerebellar White	0.392	0.361	1.387	0.850	0.005
InferiorColliculi	0.546	0.497	1.803	1.065	0.001
Thalamus	0.521	0.468	1.776	1.087	0.001

Data are mean ± SEM of 10 animals per group. *P<0.05 versus the KI hypoxia and WT hypoxia groups.
doi:10.1371/journal.pone.0108168.t001

Statistical analyses

Values are presented as mean ± SEM. Comparisons among groups were made using analysis of variance (ANOVA) or unpaired Student's t test, as appropriate. P value <0.05 was used as the cutoff for significant findings.

Results

SOD activity and quantity

Among KI adults, we found SOD activity in brain tissue was statistically significantly higher (x2) than WT adults after exposure to hypoxia (P<0.05) (Figure 1A). To find out which SOD is contributing to the increase in SOD activity, quantitative measure of SOD1, SOD2 and hSOD3 in all brain tissue was done. Our study showed that increased SOD activity after exposure to hypoxia in group KI, is mainly due to increase of both SOD2 and hSOD3 which are increased significantly in KI hypoxic group compared to RA groups and WT hypoxic group (P<0.05) (Fig. 1B). The Beta-actin promoter driving the expression of the human EC-SOD transgene did not lead to augmented expression in KI mice in response to hypoxia, but this significant augmentation in hEC-SOD protein expression in our model could by induced by other stimuli like NO [42].

Functional studies demonstrate neuronal protection in H-KI mice

PET scans showed that there was a higher uptake of ^{18}FDG in hypoxic groups compared to the normoxic groups, and the difference was statistically significant (P<0.05). Interestingly, the ^{18}FDG uptake of H-KI brains was lower than H-WT brains in areas sensitive to hypoxia, such as the hippocampus, hypothalamus, thalamus, and medulla (Figure 2 & Table 1), revealing that H-WT brains were maximally activated in their metabolism.

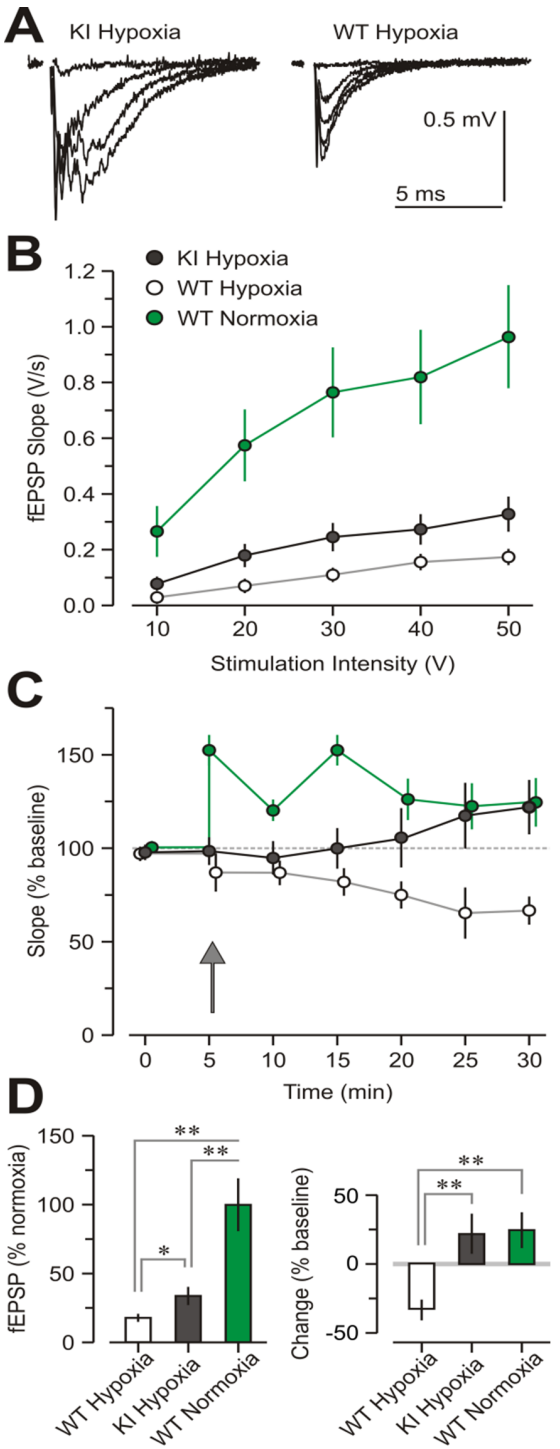

Figure 3. Hippocampal electrophysiological studies showing protected synaptic transmission and plasticity in H-KI slices, when compared to H-WT mice. (A) Representative fEPSPs of CA1 synapses at increasing stimulation strengths. (B) Input-output curves for the different groups. The slope of the fEPSPs in CA1 synapses is plotted against the stimulation intensity to the CA3 afferents. (C) Plot showing the slope of the fEPSPs, with a tetanus applied at 5 min (upward arrow) to induce LTP. (D) Bar graphs showing protection of synaptic transmission (left graph) and plasticity (right graph) in the H-KI group, when compared to the H-WT group. Notably, LTP in the H-KI group is completely normal.
doi:10.1371/journal.pone.0108168.g003

We next evaluated electrophysiological studies in *ex vivo* hippocampal measured with input-output curves for the fEPSPs of CA1 synapses, elicited by stimulation of the CA3 afferents. The data show that synaptic transmission was greatly affected in both hypoxic groups when compared to the RA-WT slices ($P<0.05$). However, the H-KI group showed significantly stronger transmission than the H-WT group ($P<0.05$), (Figure 3), suggesting that the H-WT synapses were the most affected by hypoxia. Notably, the H-KI group displayed normal long-term synaptic plasticity (LTP), because their LTP measured at 45-min post-tetanic stimulation was similar to the RA-WT group. Conversely, the H-WT slices showed complete absence of LTP (Figure 3).

Molecular studies showed attenuation of inflammatory and neural cell damage markers in H-KI mice

GSH/GSSG ratio represents the consumption of reduced glutathione due to accumulation of ROS. GSH/GSSG was significantly lower in the H-WT group compared to the H-KI group ($P<0.05$). Moreover, there was no difference between the H-KI and RA-KI groups. (Figure 4).

Next, we performed quantitative western blot analysis for inflammatory markers expressed as a ratio of protein density of each marker to Actin protein band density. GFAP expression indicates astrocytes inflammation and damage; it was statistically significantly higher in the H-WT group compared to the H-KI group ($P<0.05$). There was no difference between the H-KI and RA-KI groups. Iba1 expression, which indicates microglial cells inflammation/damage was statistically significantly higher in the H-WT group compared to the H-KI group ($P<0.05$). There was no difference between the H-KI and RA-KI groups. MIF expression as an index of systemic inflammation was statistically significantly higher in the H-WT group compared to the H-KI group ($P<0.05$). There was no difference between the H-KI and RA-KI groups. pAMPK expression as a metabolic marker, was statistically significantly higher in the H-WT group compared to the H-KI group ($P<0.05$). pACC was also significantly higher in the H-WT group compared to the other three groups, which indicates both increased amounts of pAMPK and pAMPK activity (Table 2).

Structural studies showed reduction of cell death and inflammation in H-KI mice

Caspase 3 activity, as a direct evidence of apoptosis, was significantly higher in both hypoxic groups compared to the normoxic groups ($P<0.05$). However, there was a significantly lower caspase 3 activity in the H-KI group compared to the H-WT group ($P<0.05$) (Figure 5).

Sections of the cerebrum, cerebellum or the hippocampus showed no damage (in RA groups) to minimal damage (in H-KI group). However, in the H-WT group, damage was seen in each of the cerebrum, cerebellum, and the hippocampus. Damage was very prominent in the cortical neurons of the grey matter, purkinje neurons in the cerebellum, and the neurons in the dendate gyrus of the hippocampus, which showed ischemic changes (red neuron degeneration) (Figures 6A, B & C).

Discussion

Adverse impacts of chronic or intermittent hypoxia on development, behavior, and academic achievement have been reported in many well-designed and controlled studies in children, as well as in a variety of studies in adults [43]. Hypoxia, either chronic or intermittent, has been shown to increase oxidative stress and the generation of increased superoxide anion in the brain [44–

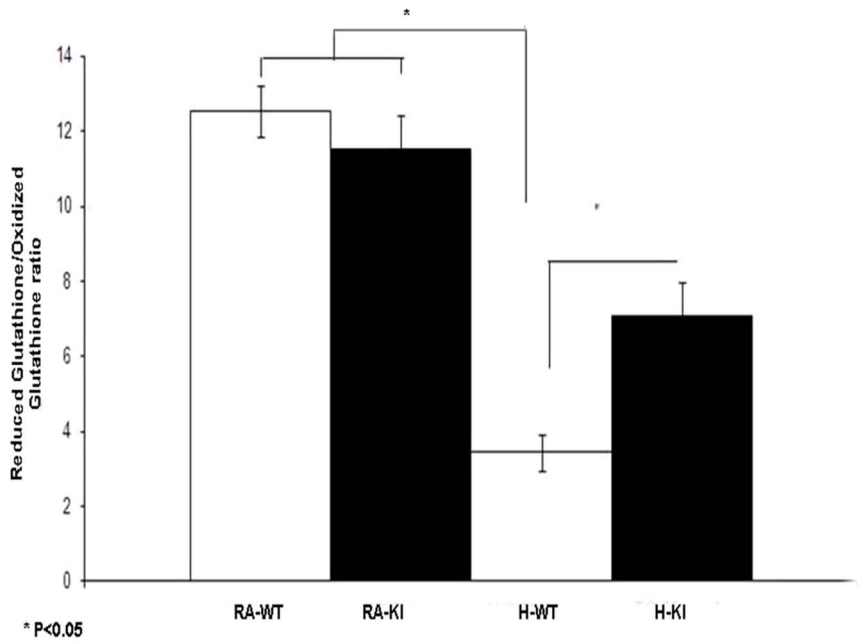

Figure 4. Reduced glutathione/oxidized ratio (GSH / GSSG) in adult mouse brain groups (WT and KI) after exposure to hypoxia (10% for 10 days) in comparison with the RA control groups (WT and KI). Data are mean of 10 animals per group ± SEM. *P<0.05 versus the KI hypoxia and WT hypoxia groups.
doi:10.1371/journal.pone.0108168.g004

45]. In this study, we showed that overexpression of EC-SOD preserved the excitatory postsynaptic potential and hippocampal neural plasticity after exposure to hypoxia compared to wild type adult mice. We also have shown a clear correlation between overexpression of EC-SOD and decreased brain damage induced by chronic hypoxia exposure as indicated by functional, molecular, and structural studies.

The protection against hypoxia-induced brain damage, offered by overexpression of EC-SOD, could be explained by different mechanisms. The oxidative stress produced by hypoxic insults leads to decreased SOD activity, increasing malondialdehyde (MDA), and lactic acid levels [46]. Inactivation of EC-SOD activity has also been shown to be associated with 100-fold elevation in hypoxia-induced Epo gene expression, compared with wild-type controls. In our KI animal model, there was marked significant increase of SOD activity when compared to WT hypoxia. It is known that human EC-SOD exists as an active and inactive isoform [47]. The marked significant increase of SOD activity in presence of little difference in the amount of EC-SOD among transgenic hypoxic animal vs. wild hypoxic animal, could be explained based on the possibility of having more active EC-SOD in the hypoxic transgenic mice and less inactive EC-SOD and this accounts for the marked change in total SOD activity. When EC-SOD was overexpressed, a significant reduction in Epo gene induction has been shown in hypoxia both *in vitro* and *in vivo* [48]. The inhibitory effect of EC-SOD on hypoxia-induced Epo expression could be due to partial stabilization of HIF-1alpha. It is known that hypoxia generated superoxide radicals are required for induction of HIF-1alpha activity and other downstream target genes [49–50]. In KI animals with overexpression of EC-SOD, dismutation of free radicals will be increased compared to the WT group. This leads to decreased levels of ROS including superoxide, which plays a major role in stabilization and activation of HIF-1alpha [51]. The resulted reduction of ROS concentration will decrease HIF-1alpha activation. Modulation of transcription

Table 2. Quantitative Assessment of Western blot for molecular markers including: GFAP, IBA1, MIF, pAMPK, and pACC in adult mouse brain groups (WT and KI) after exposure to hypoxia (10% for 10 days), in comparison with the RA control groups (WT and KI).

Markers	RA-WT	RA-KI	H-WT	H-KI
GFAP	0.792±0.04	0.796±0.03	1.426±0.08	0.812±0.08*
Iba1	0.160±0.01	0.162±0.02	0.194±0.01	0.178±0.01*
MIF	0.662±0.07	0.699±0.07	0.935±0.09	0.714±0.02*
pAMPK	0.430±0.12	0.420±0.15	1.378±0.34	0.765±0.19*
pACC	0.276±0.01	0.267±0.01	0.551±0.04	0.369±0.01*

Data are mean of 10± SEM animals per group. *P<0.05 versus the KI hypoxia and WT hypoxia groups.
* P<0.05 (H WT vs. H KI).
doi:10.1371/journal.pone.0108168.t002

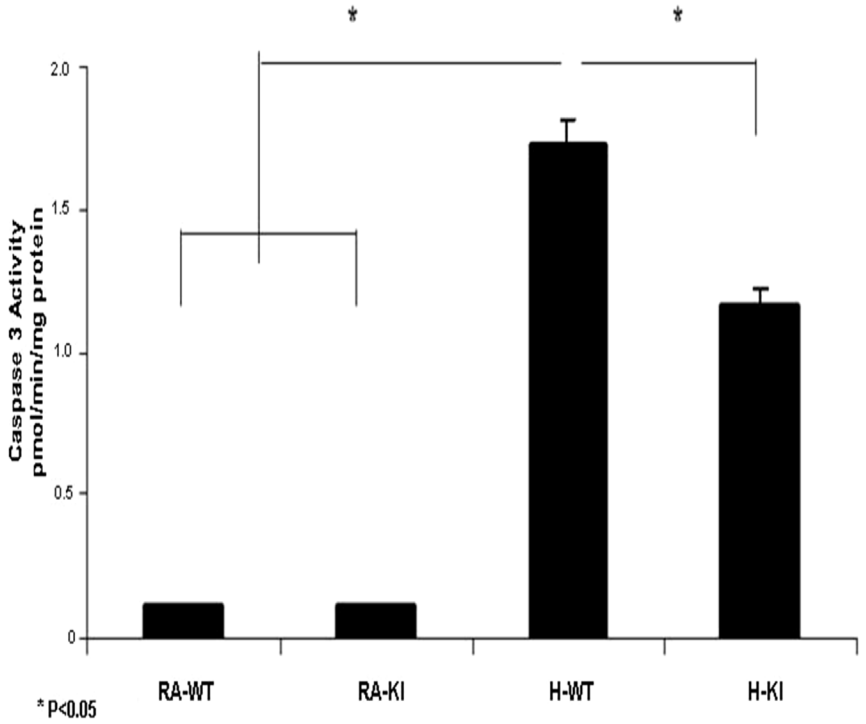

Figure 5. Activated caspase 3 ELISA in adult mouse brain groups (WT and KI), after exposure to hypoxia (10% for 10 days) in comparison with the RA control group (WT and KI). Data are mean of 10 animals per group ± SEM. *P<0.05 versus the KI hypoxia and WT hypoxia groups.
doi:10.1371/journal.pone.0108168.g005

factor HIF-1 alpha and its important gene target VEGF by the antioxidant enzyme EC-SOD was confirmed in other studies [52].

Another important mechanism, which has a great implication in explaining our findings, concerns nitric oxide (NO). NO inhibits hypoxia-inducible transcription of the Epo gene through suppression of HIF-1alpha expression, DNA binding activity, and transcriptional activity [53–54]. Under hypoxic conditions, there is a rapid accumulation of superoxide which rapidly reacts with NO to form peroxynitrite and other toxic metabolities [55–56]. In KI animals with enhanced expression of EC-SOD, superoxide is dismutated by EC-SOD to form H_2O_2. Decreased levels of superoxide would lead to increased physiologic NO concentrations and its bioavailability [57–58]. A physiological consequence of this is that EC-SOD influences blood vessel tone by maintaining the biological activity of NO [35].

With overexpression of EC-SOD and dismutation of superoxide, hydrogen peroxide accumulation is important. Many studies have handled this logical assumption by analyzing H_2O_2 in different settings. Most of the studies conclude that more SOD does not mean more H_2O_2 [59]. The formation of H_2O_2 due to dismutation of superoxide, is limited by the amount of superoxide, not by the rate it is converted to H_2O_2. Accumulation of superoxide leads to the oxidation of NO with the formation of peroxynitrite. In this situation more H_2O_2 is very unlikely to be toxic since this would amount to substituting a very mild cytotoxin (H_2O_2) for a very potent one (peroxynitrite). H_2O_2 downregulates GRK2 expression which plays a key role in G protein-coupled receptor (GPCR) signaling modulation, and its expression levels are decreased after brain hypoxia/ischemia. Therefore, pharmacological agents effective in the treatment of brain ischaemia/hypoxia should obtain an increase in the level of H_2O_2 by blocking GPx, preferably associated to an increased enzymatic activity of SOD and CAT. In the study conducted by [60], either GPx or CAT inhibition enhanced H_2O_2 toxicity in rat hippocampal slices, confirming the importance of the integrity of glial antioxidant network [61].

It has been shown that hypoxic exposure (chronic or intermittent) leads to a variety of neurological consequences which can include psychomotor impairment, learning and spatial memory impairment, and in extreme cases, memory retrieval impairment. Reaction time, total number and performance of tasks decrease significantly in hypoxic conditions, and changes in visual sensitivity, attention span, arithmetic and decision making abilities have also been noted [6],[62–64]. Imaging studies using PET imaging of H-KI and H-WT mice, showed a marked and significant reduction in FDG uptake in all scanned brain regions including brain regions sensitive to hypoxia mainly the hippocampus, hypothalamus, thalamus, and medulla (Table 1). Increases in ^{18}FDG uptake observed in specific brain regions of hypoxic animals, is generally thought to represent an increase demand in glucose metabolism from those intact cells remaining within the affected area. In fact, these alterations suggest a temporal effect of hypoxia on glucose metabolism. Finally, measurements made at times further from the initial insult may demonstrate not only greater, more widespread changes, but also marked decreases in ^{18}FDG uptake as a consequence of significant cell loss.

Electrophysiological studies showed that the H-KI group had a significantly stronger transmission than the H-WT group ($P< 0.05$), suggesting that the H-WT synapses were the most affected by hypoxia. Additionally, the H-KI group displayed normal long-term synaptic plasticity, with their LTP, measured at 45-min post-tetanic stimulation, similar to the RA-WT group. Conversely, the H-WT slices showed complete absence of LTP. Our evaluation of the hippocampal CA1-SC circuit does not include any connectiv-

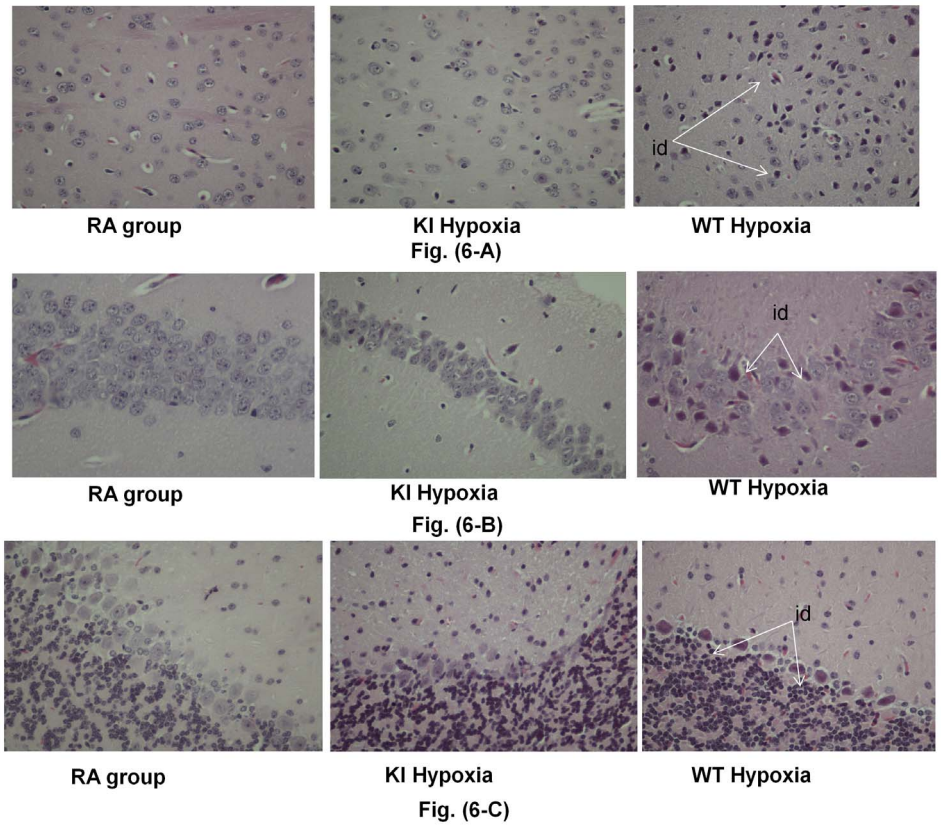

Figure 6. Brain histopathological studies of the control RA and KI hypoxia groups. (A) high-power (40X) H&E staining of cortical brains with normal structure for both the control RA and KI hypoxia groups, while the WT hypoxia group showed injury damage (id). (B) H&E, high-power (60X) view of neurons from the dentate gyrus in the hippocampus with no ischemic damage in both the control and KI hypoxia groups, while the WT hypoxia group showed injury damage (id). (C) H&E, high-power (40X) view of Purkinje cells and granular cells in the cerebellum with no ischemic damage in both the control and KI hypoxia groups, while WT hypoxia group showed injury damage (id).
doi:10.1371/journal.pone.0108168.g006

ity data, such as synaptic counts, though we believe that this data might add to our understanding of the role of EC-SOD in hippocampal function. This finding could explain the deterioration of both learning and memory in WT mice after exposure to hypoxia and also shows the protective effect of overexpression of EC-SOD in the KI mice group (Fig. 2). We believe that it is the first time that the protective effect of overexpression of EC-SOD has been reported in this setting.

Hypoxic exposure results in a significant increase in pro-inflammatory cytokines including MIF [2]. In neonatal rats with hypoxia-ischemia brain damage, there was a marked increase in the expression of MIF in the brain [64]. In the murine brain, MIF transcripts and protein are mainly present in the cortex, hippocampus, and pituitary gland [65]. In our study there was a significantly marked reduction of MIF expression in brain tissue of H-KI mice compared to the H-WT group (Table 2). This finding supports the anti-inflammatory function of EC-SOD, which could be explained by down regulation of HIF-1alpha and inactivation of NF-KB [55,66]. In our previous studies, we showed that overexpression of EC-SOD inhibits activation of NF-KB induced by increased ROS in our *in vitro* model [57],[67]. Decreased brain cell inflammation/damage induced by hypoxia was significantly prominent by the significant decrease in the studied inflammatory markers including GFAP, IBA1, and MIF.

In summary, overexpression of EC-SOD and increased its activity has a significant protective effect against chronic hypoxia-induced brain damage. A therapeutic approach that increases EC-SOD protein accumulation, either by overexpression or a therapeutic supplement, could be used prophylactically in patients with long term pathological conditions and chronic disease such as COPD, pulmonary hypertension, sleep disordered breathing and sickle cell disease, all of which are associated with compromised brain oxygenation. A similar approach may also be useful in situations such as hypoxic ischemic insult of newborn, sickle cell disease, stroke or drowning, all of which can lead to impairment of brain function, including learning and spatial memory impairment and psychomotor impairment. Additionally, such a regime could be used as a protective measure for individuals who are operating at the limits of human tolerance and facing relevant operational stressors such as hypoxia, a significant physiological threat at altitude.

Author Contributions

Conceived and designed the experiments: NZ PM EM MA. Performed the experiments: NZ HP CC SD SF MN. Analyzed the data: NZ SD PH MA. Contributed reagents/materials/analysis tools: PM SD EM MA. Wrote the paper: NZ EM MN MA.

References

1. Carvalho C, Santos MS, Baldeiras I, Oliveira CR, Seiça R, et al. (2010) Chronic hypoxia potentiates age-related oxidative imbalance in brain vessels and synaptosomes. Curr Neurovasc Res 7(4)288–300.
2. Himadri P, Kumari SS, Chitharanjan M, Dhananjay S (2010) Role of oxidative stress and inflammation in hypoxia-induced cerebral edema: a molecular approach. High Alt Med Biol 1: 231–44.
3. Lu Q, Mark SW, Harris VA, Aggarwa lS, Hou Y, et al. (2012) Increased NADPH oxidase derived superoxide is involved in the neruonal cell death induced by hypoxia ischemia in neonatal hyppocampal slice cultures. Free Radical biol Med 53(5): 1139–1151.
4. Ten VS, Yao J, Ratner V, Sosunov S, Fraser DA, et al. (2010) Complement ComponentC1q Mediates Mitochondria-Driven Oxidative Stress in Neonatal Hypoxic–Ischemic Brain Injury. The Journal of Neuroscience 30: 2077–2087.
5. Jin K, Sun Y, Xie L, Peel A, Mao XO, et al. (2003) Directed migration of neuronal precursors into the ischemic cerebral cortex and striatum. Mol. Cell. Neurosci 24: 171–189.
6. Paola MD, Caltagirone C, Fadda L, Sabatini U, Serra L, et al. (2008) Hippocampal Atrophy Is the Critical Brain Change in Patients With Hypoxic Amnesia. Hippocampus 18: 719–728.
7. Ahmed MN, Veber V, Hogg N, Auten RL (2004) Overexpression of Extracellular Superoxide Dismutase (EC-SOD) Prevents Lipid Peroxidation in Hyperoxia-Exposed Newborn Mouse Lung. Ped. Res. A: No.2592.
8. Wang J, Wen L, Huang Y, Chen Y, Ku M (2006) Dual Effects of Antioxidants in Neurodegeneration: Direct Neuroprotection against Oxidative Stress and Indirect Protection via Suppression of Glia mediated Inflammation. Current Pharmaceutical Design 12: 3521–3533.
9. Lee HM, Greeley GH, Englander EW (2008) Sustained hypoxia modulates mitochondrial DNA conent in the neonatal rat brain. Free Radic Biol Med 44(5): 807–814.
10. Veasey S, Davis CW, Fenik P, Zhan G, Hsu Y, et al. (2004) Long-term Intermittent Hypoxia in Mice: Protracted Hypersomnolence with Oxidative Injury to Sleep-Wake Brain Regions. Sleep 27(2): 194–201.
11. Emerit J, Edeas M, Bricaire F (2004) Neurodegenerative diseases and oxidative stress. Biomed. Pharmacother 58: 39–46.
12. Halliwell B (2001) Role of free radicals in the neurodegenerative diseases: therapeutic implications for antioxidant treatment. Drugs Aging. 18: 685–716.
13. Chávez JC, Agani F, Pichiule P, LaManna JC (2000) Expression of hypoxia-inducible factor-1alpha in the brain of rats during chronic hypoxia. J Appl Physiol 89: 1937–42.
14. Sutter CH, Laughner E, Semenza GL (2000) Hypoxia-inducible factor 1α protein expression is controlled by oxygen-regulated ubiquitination that is disrupted by deletions and missense mutations. Proc Natl Acad Sci USA 97: 4748–4753.
15. Brahimi-Horn MC, Pouyssegur J (2007) Harnessing the hypoxiainducible factor in cancer and ischemic disease. Biochem Pharmacol 73: 450–457.
16. Floyd R (1999) Antixociants, oxidative stress and degebnrative disorders. Exp Boil Med 222: 236–245.
17. Bickler PE, Fahlman CS (2004) Moderate increases in intracellular calcium activate neuroprotective signals in hippocampal neurons. Neuroscience 127: 673–83.
18. Bickler PE, Fahlman CS (2010) Hypoxic preconditioning failure in aging hippocampal neurons: impaired gene expression and rescue with intracellular calcium chelation. J Neurosci Res 88: 3520–9.
19. Bickler PE (2004) Clinical perspectives: neuroprotection lessons from hypoxia-tolerant organisms. J of Experimen Biol 207: 3243–3249.
20. Klaunig JE, Kamendulis LM, Hocevar BA (2010) Oxidative Stress and Oxidative Damage in Carcinogenesis. Toxicologic Pathol 38: 96–109.
21. Yang G, Chan PH, Chen J, Carlson E, Chen SF, et al. (1994) Human copper-zinc superoxide dismutase transgenic mice are highly resistant to reperfusion injury after focal cerebral ischemia. Stroke 25: 165–170.
22. Noshita N, Sugawara T, Hayashi T, Lewén A, Omar G, et al. (2002) Copper/zinc superoxide dismutase attenuates neuronal cell death by preventing extracellular signal-regulated kinase activation after transient focal cerebral ischemia in mice. J Neurosci 22: 7923–7930.
23. Fujimura M, Morita-Fujimura Y, Noshita N, Sugawara T, Kawase M, et al. (2000) The cytosolic antioxidant copper/zincsuperoxide dismutase prevents the early release of mitochondrial cytochrome c in ischemic brain after transient focal cerebral ischemia in mice. J Neurosci 20: 2817–2824.
24. Sugawara T, Noshita N, Lewén A, Gasche Y, Ferrand-Drake M, et al. (2002) Overexpression of copper/zinc superoxide dismutase in transgenic rats protects vulnerable neurons against ischemic damage by blocking the mitochondrial pathway of caspase activation. J Neurosci 22: 209–217.
25. Narasimhan P, Fujimura M, Noshita N, Chan PH (2003) Role of superoxide in poly(ADP-ribose) polymerase upregulation after transient cerebral ischemia. Brain Res Mol Brain Res 113: 28–36.
26. Kim GW, Kondo T, Noshita N, Chan PH (2002) Manganese superoxide dismutase deficiency exacerbates cerebral infarction after focal cerebral ischemia/reperfusion in mice: implications for the production and role of superoxide radicals. Stroke 33: 809–815.
27. Zhou M, Dominguez R, Baudry M (2007) Superoxide dismutase/catalase mimetics but not MAP kinase inhibitors are neuroprotective against oxygen/glucose deprivation-induced neuronal death in hippocampus. J Neurochem 103: 2212–2223.
28. Marklund SL (1983) Extracellular superoxide dismutase in human tissues and human cell lines. J Clin Invest 74: 1398–1403.
29. Oury TD, Ho YS, Piantadosi CA, Crapo JD (1992) Extracellular superoxide dismutase, nitric oxide, and central nervous system O2 toxicity. Proc Natl Acad Sci USA 89: 9715–9719.
30. Oury TD, Card JP, Klann E (1999) Localization of extracellular superoxide dismutase in adult mouse brain. Brain Res 850: 96–103.
31. Oury TD, Day BJ, Crapo JD (1996) Extracellular superoxide dismutase in vessels and airways of humans and baboons. Free Radic Biol Med 20: 957–65.
32. Sheng H, Bart RD, Oury TD, Pearlstein RD, Crapo JD, et al. (1999a) Mice overexpressing extracellular superoxide dismutase have increased resistance to focal cerebral ischemia. Neuroscience 88: 185–19.
33. Sheng H, Bart RD, Oury TD, Pearlstein RD, Crapo JD, et al. (1999b) Mice overexpressing extracellular superoxide dismutase have increased tolerance to global cerebral ischemia. Exp Neurol 163: 392–398.
34. Sheng H, Brody T, Pearlstein RD, Crapo J, Warner DS (1999c) Extracellular superoxide dismutase deficient mice have decreased resistance to focal cerebral ischemia. Neurosci Lett 267: 13–17.
35. Demchenko IT, Oury TD, Crapo JD, Piantadosi CA (2002) Regulation of the Brain's Vascular Responses to Oxygen. Circ Res 91: 1031–1037.
36. Ahmed MN, Suliman H, Folz R, Grayck EN, Auten RL (2003) Extracellular superoxide dismutase protects lung development in hyperoxic newborn mice. Am J Resp Crit Care Med 167: 440–445.
37. Ahmed MN, Zhang Y, Codipilly C, Zaghloul N, Patel D, et al. (2012) EC-SOD overexpression can reverse the course of hypoxia-induced pulmonary hypertension in adult mice. Mol Med 18: 38–46.
38. Zaghloul N, Nasim M, Patel H, Codipilly C, Marambaud P, et al. (2012) Overexpression of EC- SOD has a protective role against hyperoxia induced brain injury in neonatal mice. FEBS 279: 871–881.
39. Chang EH, Savage MJ, Flood DG, Thomas JM, Levy RB, et al. (2006) AMPA receptor downscaling at the onset of Alzheimer's disease pathology in double knockin mice. Proc Natl Acad Sci USA 103: 3410–3415.
40. Hissin PJ, Hilf R (1976) A fluorometric method for determination of oxidized and reduced glutathione in tissues. Anal Biochem 74: 214–226.
41. Han BH, D'Costa A, Back SA, Parsadanian M, Patel S, et al. (2000) BDNF blocks caspase-3 activation in neonatal hypoxia–ischemia. Neurobiol Dis 7: 38–53.
42. Fukai T, Siegfried MR, Ushio-Fukai M, Cheng Y, Kojda G, et al. (2000) Regulation of the vascular extracellular superoxide dismutase by nitric oxide and exercise training. J Clin Invest 105: 1631–1639.
43. Bass JL, Corwin M, Gozal D, Moore C, Nishida H, et al. (2004) The Effect of Chronic or Intermittent Hypoxia on Cognition in Childhood: A Review of the Evidence. Pediatrics 114: 05–816.
44. Fabian RH, Perez-Polo JR, Kent TA (2004) Extracellular superoxide concentration increases following cerebral hypoxia but does not affect cerebral blood flow. Int J Dev Neurosci 22: 225–30.
45. Xu W, Chi L, Row BW, Xu R, Ke Y, et al. (2004) Increased oxidative stress is associated with chronic intermittent hypoxia-mediated brain cortical neuronal cell apoptosis in a mouse model of sleep apnea. Neuroscience 126: 313–23
46. Dingyu H, Qin L, Bo L, Rongji D, Lina G, et al. (2009) Stress Response to Hypoxia in Wistar Rat: LA, MDA, SOD and Na+-K+-ATPase. Bioinformatics and Biomedical Engineering 20 Available: www.lw20.com09. ICBBE.
47. Petersen SV, Kristensen T, Petersen JS, Ramsgaard L, Oury TD, et al. (2008) The Folding of Human Active and Inactive Extracellular Superoxide Dismutases Is an Intracellular Event. J. Biol. Chem. 283(22):15031–36.
48. Zelko IG, Folz RJ (2004) Extracellular Superoxide Dismutase Functions as a Major Repressor of Hypoxia-Induced Erythropoietin Gene Expression. Endocrinol 146: 332–340.
49. Chandel NS, Maltepe E, Goldwasser E, Mathieu CE, Simon MC, et al. (1998) Mitochondrial reactive oxygen species trigger hypoxia-induced transcription. Proc Natl Acad Sci USA 95: 11715–11720.
50. Agani FH, Pichiule P, Chavez JC, LaManna JC (2000) The role of mitochondria in the regulation of hypoxia-inducible factor-1 expression during hypoxia. J Biol Chem 275: 35863–35867.
51. Zagórska A, Dulak J (2004) HIF-1: the knowns and unknowns of hypoxia sensing. Acta Biochimica Polonica 51: 563–585.
52. Sibenalle ZA, Welsh JL, Du C, Witmer JR, Schrock HE, et al. (2014) Extracellular superoxide dismutase suppresses hypoxia-inducible factor-1α in pancreatic cancer. Free Radical Biology and Medicine 69: 357–366.
53. Sogawa K, Sogawa K, Numayama-Tsuruta K, Ema M, Abe M, et al. (1998) Inhibition of hypoxia-inducible factor-1 activity by nitric oxide donors in hypoxia. Proc Natl Acad Sci USA 95: 7368–7373.
54. Huang LE, Willmore WG, Gu J, Goldberg MA, Bunn HF (1999) Inhibition of hypoxia-inducible factor 1 activation by carbon monoxide and nitric oxide. Implications for oxygen sensing and signaling. J Biol Chem 74: 9038–9044.
55. Brown GC (2007) Mechanisms of inflammatory neurodegeneration: iNOS and NADPH oxidase. Biochem Soc Trans 35: 1119–1121.

56. Zhan G, Serrano F, Fenik P, Hsu R, Kong L, et al. (2005) NADPH oxidase mediates hypersomnolence and brain oxidative injury in a murine model of sleep apnea. Am J Respir Crit Care Med 172: 921–929.
57. Ahmed MN, Codipilly C, Hogg A, Auten RL (2011) The protective effects of overexpression of extracellular superoxide dismutase on nitric oxide bioavailability in the lung after exposure to hyperoxia stress. Exp Lung Res 37: 10–7.
58. Ortega MA, de Artinano AA (2000) Nitric oxide reactivity and mechanisms involved in its biological effects. Pharmacol Res 42: 421–427.
59. Lin MT and Beal MF (2006) Mitochondrial dysfunction and oxidative stress in neurodegenerative diseases. Nature 443: 787–795.
60. Avshalumov MV, MacGregor DG, Sehgal LM, Rice ME (2004) The glial antioxidant network and neuronal ascorbate: protective yet permissive for H_2O_2 signaling. Neuron Glia Biol 1: 365–376.
61. Armogida M, Nisticò R, Mercuri NB (2011) Therapeutic potential of targeting hydrogen peroxide metabolism in the treatment of brain ischaemia. B.J. Pharm 166: 1211–1224.
62. Cervos-Navarro J, Sampaolo S, Hamdorf G (1991) Brain changes in experimental chronic hypoxia. Exp Pathol 42: 205–12.
63. Jin K, Mao XO, Sun Y, Xie L, Greenberg DA (2002) Stem cell factor stimulates neurogenesis in vitro and in vivo. J Clin Invest 110: 311–9.
64. Wang LL, Guo WJ, Du WN (2011) Study on the expression and the role of macrophage migration inhibitory factor in the brain of neonatal rats with hypoxia-ischemia brain damage. Sichuan Da Xue Xue Bao Yi Xue Ban 42: 199–203.
65. Bacher M, Meinhardt A, Lan HY, Meinhardt A, Lan HY, et al. (1998) MIF expression in the rat brain: implications for neuronal function. Mol Med 4: 217–230.
66. Kim Y, Kim BH, Lee H, Jeon B, Lee YS, et al. (2011) Regulation of skin inflammation and angiogenesis by EC-SOD via HIF-1alpha and NF-KB pathways. Free Rad Biol & Med 51: 1985–1995.
67. Oury TD, Day BJ, Crapo JD (1996) Extracellular superoxide dismutase: a regulator of NO bioavailability. Lab Invest 75: 617–636.